



Published in final edited form as:

Pediatr Res. 2021 May ; 89(6): 1389–1395. doi:10.1038/s41390-020-01156-0.

Bilirubin inhibits lipid raft dependent functions of L1 cell adhesion molecule in rat pup cerebellar granule neurons

Spencer T. Kitchen¹, Ningfeng Tang², Min He³, Eric Ly⁴, Sandra M. Mooney⁵, Cynthia F. Bearer^{1,*}

¹Department of Pediatrics, Case Western Reserve University School of Medicine, Cleveland, Ohio, 44106

²Department of Orthopedics, University of Maryland School of Medicine, Baltimore, Maryland, 21201

³Department of Pathology, Johns Hopkins University School of Medicine, Baltimore, Maryland, 21218

⁴Division of Neonatology, University of Maryland School of Medicine, Baltimore, Maryland, 21201

⁵Department of Nutrition, University of North Carolina School of Public Health, Chapel Hill, North Carolina, 27514

Abstract

Background: The mechanism of bilirubin neurotoxicity is poorly understood. We hypothesize that bilirubin inhibits the function of lipid rafts (LR), microdomains of the plasma membrane critical for signal transduction. To test this hypothesis, we measured the effect of free bilirubin (Bf) between 7.6 – 122.5 nM on LR dependent functions of L1 cell adhesion molecule (L1).

Methods: Cerebellar granule neurons (CGN) were plated on poly L-lysine overnight, and neurite length was determined after 1 h treatment with L1 alone or L1 and bilirubin. L1 activation of ERK1/2 was measured in CGN in the presence or absence of bilirubin. The effect of bilirubin on L1 distribution in LR was quantitated, and the localization of bilirubin to LR was determined.

Results: The addition of bilirubin to CGN treated with L1 significantly decreased neurite length compared to L1 alone. L1 activation of ERK1/2 was inhibited by bilirubin. Bilirubin redistributed

Users may view, print, copy, and download text and data-mine the content in such documents, for the purposes of academic research, subject always to the full Conditions of use:http://www.nature.com/authors/editorial_policies/license.html#terms

*Corresponding author: Cynthia F. Bearer, M.D., Ph.D., Department of Pediatrics, 2109 Adelbert Rd, 8th floor, Cleveland, OH 44106, Tel. (410) 328-6003, Fax. (410) 328-1076, Cynthia.Bearer@uhhospitals.org.

Spencer T. Kitchen substantially contributed to the analysis and interpretation of data, and drafting and revising of this article.

Ningfeng Tang substantially contributed to the design of this study and the acquisition and analysis of data in this article.

Min He substantially contributed to the design of this study and the acquisition and analysis of data in this article.

Eric Ly substantially contributed to the drafting of this article and the acquisition of data in this article.

Sandra M. Mooney substantially contributed to the design of this study and the revising of this article.

Cynthia F. Bearer substantially contributed to the conception and design of this study and has final approval of the version to be published.

Category of Study: Basic science

Disclosure. The authors declare no conflict of interest in the article.

No patient consent was required for this study.

L1 into LR. Bilirubin was associated only with LR containing fractions of a sucrose density gradient.

Conclusion: Bf significantly inhibits LR-dependent functions of L1 and are found only associated with LR suggesting one mechanism by which bilirubin may exert neurotoxicity is through the dysfunction of protein-LR interactions.

INTRODUCTION

Bilirubin has long been associated with cerebellar dysfunction, which can result in dystonia in full term and premature newborns (1). Neurotoxicity has been seen to occur in premature infants at much lower levels of bilirubin compared to full term infants (2), indicating increased susceptibility. Premature neonates (<35 weeks gestation) may be at increased risk (3) because cerebellar development is particularly vulnerable in preterm neonates (4). Although phototherapy is the current standard for treatment of hyperbilirubinemia, reduction of total serum bilirubin (TSB) does not adequately correlate with a reduction in bilirubin neurotoxicity (5). Mounting evidence suggests that the unbound fraction of bilirubin (free bilirubin (Bf)) is important in predicting bilirubin neurotoxicity (6–9). A meta-analysis of *in vitro* studies shows that Bf induces apoptosis and reduces cellular proliferation in neurons (10) indicating a more direct effect on neural development than total bilirubin. Bf binds to neuronal membranes (11) and to phospholipids (12,13). However, currently there are no studies on Bf binding capabilities to different phospholipids.

There is growing recognition that lipid membrane composition plays a key role in cell physiology. While studies of protein ion channels commonly treat the plasma membrane as a simple inert supporting layer, studies reveal that lipids themselves play important biological roles as direct signaling elements (14,15) and protein ion channel regulators (16,17). Wide ranges of protein ion channels associate with specific lipid microdomains (18), with regulation of channel conductance resulting from protein interactions with the lipids as well as changes in the physical properties of the membrane (19). In particular, membrane microdomains containing specific phospholipids, termed lipid rafts (LR), float freely in the membrane, but with the proper stimulus, form ordered and tightly packed structures within the bilayer (14,20). The past decade reveals that LR play a number of important physiological functions and compartmentalize cellular processes by influencing membrane fluidity, recruiting and organizing the assembly of signaling molecules, affecting the trafficking of membrane proteins, and regulating neurotransmission and receptor transport (21–23).

Because bilirubin binds to phospholipids, we hypothesized that bilirubin binds to and causes LR dysfunction. L1 cell adhesion molecule (L1) is dependent on LR to mediate neurite outgrowth, whereas laminin mediates neurite outgrowth through a LR-independent mechanism (24,25). L1 only briefly traffics through LR in the growth cone during the endocytic recycling process necessary for neurite outgrowth (26). Non-lipid raft L1 is found in the plasma membrane and is used to promote nerve fasciculation. Ethanol has been shown to increase the fraction of L1 found in LR leading to impairment of LR mediated neurite outgrowth (25). L1 initiates a signaling pathway that leads to activation of p60src,

a constitutive LR protein, and ERK1/2 (27). Inhibition of p60src reduces L1 activation of ERK1/2 (28). Inhibition of ERK1/2 decreases neurite length of neurons grown in the presence of L1 (27). Thus, dysfunction of LR will reduce L1-, but not laminin-, mediated neurite outgrowth, as well as decrease L1 activation of ERK1/2. We test our hypothesis using cerebellar granule neurons (CGN) from postnatal day 5 rat pups (day of birth is postnatal day 0), a well-established and relevant model of human brain growth during the third trimester (29–31) and a well described model of bilirubin neurotoxicity (32).

METHODS

Antibodies and materials:

Mouse monoclonal anti-beta III tubulin were obtained from Sigma (St. Louis, MO) (catalog #T8660), and goat anti mouse IgG (heavy and light chain) conjugated to Alexa 488 was obtained from Invitrogen (Grand Island, NY) (catalog #A11001). Rabbit polyclonal antibody against dually phosphorylated activated ERK1/2 (catalog #9101) and rabbit polyclonal antibodies against total ERK (catalog #9102) were obtained from Cell Signaling (Beverly, MA, USA). Rabbit polyclonal antibody to mouse IgG (catalog #315–005-003), and rabbit polyclonal antibody to mouse IgG (H+L) conjugated to hydrogen peroxidase (catalog #315–035-003) were obtained from Jackson Immuno-Research (West Grove, PA, USA). Mouse monoclonal antibody to rat L1 (ASCS4) was obtained from the Developmental Studies Hybridoma Bank developed under the auspices of the NICHD and maintained by The University of Iowa, Department of Biology, Iowa City, IA 52242. Horseradish peroxidase (HRP)-conjugated cholera toxin B subunits (CTXB) were purchased from Sigma (catalog #C3741–1VL). Goat polyclonal anti-neural cell adhesion molecule L1 polyclonal antibody to the cytoplasmic domain of L1 (anti-L1CD) was obtained from Santa Cruz Biotechnology (Santa Cruz, CA) (catalog #sc-374046). Rabbit polyclonal anti-bilirubin antibody was obtained from Biomatik (Wilmington, DE), capable of detecting total bilirubin (catalog #CAU21553). Methyl beta cyclodextrin (MBCD) was obtained from Sigma. The substrates used for these experiments were 0.1% poly L-lysine (PLL) (Sigma), laminin (Lam) (Invitrogen), and L1-Fc, a soluble chimeric protein consisting of the extracellular domain of L1 cell adhesion molecule and the Fc domain of IgG (purchased from R&D Systems as a 20 µg/ml solution, Minneapolis, MN). Bilirubin, horseradish peroxidase and human serum albumin (HSA) were obtained from Sigma.

Bilirubin Preparation:

Immediately before each experiment, bilirubin was dissolved in 0.1 M NaOH and stabilized with 100 µM HSA. This solution was then diluted in K5 media to yield final bilirubin concentrations of 5, 10, and 50 µM to be added to tissue culture wells. The solution was prepared in the dark to limit bilirubin photo-isomerization due to light. All cultures containing bilirubin were kept in the dark.

Measurement of Bf concentrations:

The peroxidase-diazo method revised from Ahlfors (33) was used to determine the concentration of Bf immediately after preparation of the 5, 10, and 50 µM bilirubin samples in K5 media alone, to characterize the initial conditions that neurons experience.

The competitive inhibition constant (K_p) for horseradish peroxidase (HRP) (Sigma) was calculated from the reaction rate of enzymatic oxidation of Bf with hydrogen peroxide (Sigma). Albumin-bound bilirubin was unable to participate in the oxidation reaction and was left unchanged in the solution. Oxidized Bf was unable to be diazotized. Bf in the samples was oxidized using HRP; the remaining unoxidized bilirubin in the samples was diazotized. This diazotization allowed the unoxidized, albumin-bound bilirubin to be measured spectrophotometrically, quantified, and compared to the total unconjugated bilirubin before oxidation. Bf concentrations in the samples were calculated from the difference of total starting bilirubin and the diazotized bilirubin that remained in the reactions with different HRP concentrations (34).

The concentrations of Bf in the HSA containing media were: 7.6, 37.6, and 122.5 nM in 5, 10, and 50 μ M total bilirubin solutions respectively. Both 7.6 and 37.6 are concentrations of Bf in the physiologic range.

Cell Cultures:

CGN from 5 day-old Sprague-Dawley rat pups were prepared as previously described (25,28,35). All pups in each litter were used, and cell cultures were a mix of male and female pups. To minimize pain and discomfort, the pups were rapidly decapitated as approved by the University of Maryland School of Medicine Institutional Animal Care and Use Committee. Cerebella were dissected and suspended in ice cold PBS buffer, then trypsinized to prepare a single cell suspension. Viability of CGN was assessed with trypan blue and was routinely >90%. The CGN suspension was diluted to a concentration of 2×10^4 cells/mL and plated with Neurobasal media (Gibco, Rockville, MD) which contained the following additions: 2% B27 supplement (Gibco), 2 mM L-glutamine, 6 g/L glucose, 20 mM HEPES, pH 7.2, and 1% penicillin/streptomycin (referred to as K5). All treatment conditions for experiments in this study contained 100 μ M de-lipidated human serum albumin (HSA) to control for unbound albumin in the bilirubin solutions. All CGN were grown on surfaces treated with PLL. Some glass coverslips were treated with laminin beforehand, and some cells were plated with L1-Fc supplemented K5 media.

Preparation of growth substrate:

Coverslips obtained from Fisher Scientific (Hanover Park, IL) were cleaned and placed in the bottom of each of a 24 well Costar tissue culture flat bottom plate. Into each of the 24 wells was placed one mL ice cold 0.1% poly L-lysine (PLL). They were then sealed and placed in the refrigerator at 4°C overnight. L1 containing wells were prepared as follows: Just prior to the addition of CGN, the PLL solution was removed from the wells and each well was washed in ice cold PBS three times. Into each well was added 0.5 mL of pre-warmed K5 media and 10 μ l of a 20 μ g/ml solution of L1-Fc to give a concentration of 0.4 μ g/mL (25,30,31). Prepared CGN suspension was added to bring the total volume in each well to 1 mL. Laminin containing wells were prepared as follows: The PLL solution was removed from the wells, each well was washed in ice cold phosphate buffered saline (PBS) three times, then 1 mL of a 2 mg/mL laminin solution in PBS was added to each well. The plate was again sealed and placed in the refrigerator overnight at 4°C. Just prior to addition of CGN, the laminin solution was removed from the wells (30,35). Into each well

was added 0.5 mL of pre-warmed K5 media and prepared CGN suspension to bring the total volume in each well to 1 mL.

Neurite outgrowth:

For neurite outgrowth experiments, CGN cultures grown on PLL or laminin, or treated with L1-Fc were incubated for 2 h at 37°C in 10% CO₂ to allow cell adhesion. Bilirubin-containing media was added in the dark, 2 h after plating. Cells were grown for 22 h after bilirubin treatment in a humid atmosphere of 90% air, 10% CO₂ at 37°C in the dark. At 22 h there was no change in cell density and cells did not appear pyknotic.

The media was removed and cells were washed X3 with ice cold PBS. The cells were then fixed in 4% paraformaldehyde for 30 min at room temperature, followed by X3 washes with PBS. Blocking solution (3% BSA/0.2% Triton X-100/PBS) was added to each coverslip for 30 min at 37°C, or overnight at 4°C. Blocked cells were exposed to mouse monoclonal anti-tubulin beta III for 2 h at 37°C. Following primary antibody exposure, the coverslips were washed 3X with PBS and then exposed to the secondary antibody, Alexa 488 anti-mouse IgG for 1 h at 37°C. Finally, the wells were washed X3 with PBS, and mounted on glass slides. Cells were viewed on a Zeiss Observer Z1 fluorescence inverted microscope at objective 20X (Carl Zeiss Microscopy, LLC). Images were captured using Axiovision camera software (Carl Zeiss Oberkochen, Germany), and neurite outgrowth was measured using Image J software (National Institutes of Health, Bethesda, MD). Eligible neurites were identified by a masked investigator in an *a priori* design. Eligible neurons were photographed and neurite length measured. Neurite length was measured as the distance between the center of the cell soma and the tip of its longest neurite. Only neurons containing neurites that met the following criteria were measured: 1) The neurite was at least as long as the width of soma; 2) The neurite was not touching another neuron; 3) The neuron was single and not in a cluster (25,35). Slides were scanned for eligible neurons from left to right until at least 30 neurites from each coverslip were identified and photographed for measurement.

L1 activation of ERK1/2 in the presence or absence of MBCD:

The ability of L1 to activate ERK1/2 in the absence of LR was tested with MBCD, which chelates cholesterol and disperses LR. We have previously shown that the addition of 4 mM MBCD to CGN for 1 h dissolves LR without affecting cell viability (25). ERK1/2 was activated by addition of a cross-linked anti-L1 monoclonal antibody, ASCS4, as previously described (27,36). ASCS4 was cross-linked by mixing with rabbit anti-mouse IgG (H+L) (1:2.5 g/g) to form multimeric complexes (clASCS4). The mixture was incubated for 1 h at 4°C prior to addition to cells. Mouse IgG was used as the positive control. Cells were plated on PLL in K5 media at 2×10^5 and grown overnight in 10% CO₂ at 37°C. After 24 h of incubation, media was replaced with fresh pre-warmed K5 media, and either bilirubin media (5, 10, or 50 µM prepared as for NOG experiment) or 4 mM MBCD with 0.02% DMSO added to the cultures. The prepared cross-linked ASCS4 or mouse IgG was added 1 h after the addition of bilirubin or MBCD. Cells were washed with ice-cold Hank's balanced salt solution (HBSS) 10 min after addition of cross-linked ASCS4 or mouse IgG. Cells were then scraped from dishes and incubated with lysis buffer for 30 min, followed by a

centrifugation of 10,000 g for 10 min at 4°C. Cell lysates were boiled for 5 min in Laemmli sample buffer, run on SDS-PAGE (12% gel) and western blotted as described below.

Determination of L1 distribution in LR:

CGN were plated on 100 mm dishes at a density of 6×10^6 in K5 media and incubated in 10% CO₂ at 37°C overnight. The media was replaced with fresh prewarmed K5 media three h prior to harvest. Half of the K5 media was removed and replaced one h prior to harvest, with either bilirubin media (final concentration 5 μM, prepared the same as for NOG), ethanol (25 mM) as a positive control (25), or HSA media alone to serve as a negative control. Cultures were kept in a dark incubator. All equipment was cooled to 4°C. The media was removed and cells were washed with cold HBSS. CGN were scraped and lysed in low detergent buffer consisting of 20 mM Tris, pH 7.4, 150 mM NaCl, 0.5% Triton X-100, 10% glycerol, 10 mM Na-vanadate, 2 μM aprotinin, 0.1 mM phenylmethylsulfonyl fluoride, 1 μM leupeptin, 1 μg/mL pepstatin A, 10 μg/mL turkey trypsin inhibitor, 100 pM cypermethrin, phosphatase inhibitor cocktail I (Sigma), and phosphate inhibitor cocktail II (Sigma). The lysates were centrifuged for 30 min at 13,000 g at 4°C. After centrifugation, 2 mL of the lysate supernatant was mixed with an equal volume of 80% sucrose solution and then overlaid by a sucrose density gradient with 32% and 5% layers. The gradient was centrifuged at 180,000 g, for 24 h at 4°C. Sequential 1 mL fractions were drawn off the top of the gradient. Fractions containing LR were identified by dot blots for cholera toxin subunit B reactivity as described below. Proteins from an equivolume of each LR and non-LR pool (bilirubin, ethanol, and control) were precipitated using chloroform/methanol and resuspended in Laemmli sample buffer and run on SDS-PAGE, followed by immunoblotting as described below.

Dot Blots:

Two μL aliquot from each fraction (generated above) was blotted onto a nitrocellulose membrane. After drying, the dot blots were blocked with 5% BSA for 1 h and then incubated with the primary detector for 30 min, with either anti-bilirubin to detect bilirubin or CTXB conjugated to HRP to detect GM1 ganglioside. After washing with TBS, the blots made with the bilirubin antibody were incubated with rabbit polyclonal antibody to mouse IgG (H+L) conjugated to hydrogen peroxidase for 30 min and then washed with TBS again. Blots were incubated with ECL reagents for 1 min, and then dot blot images were captured using x-ray film.

Western blots:

The samples were separated by SDS-PAGE (12% gel) and transferred to a polyvinylidene difluoride membrane. The membrane was blocked in Tris-buffered saline containing 2% bovine serum albumin (BSA) and 0.1% Tween-20. The membrane was incubated with antibodies to dually phosphorylated ERK1/2 or the cytoplasmic domain of L1 (L1-CD) and HRP-conjugated CTXB. The membrane was then washed and probed with HRP-goat anti-rabbit IgG, then reactive proteins were visualized by chemiluminescence. Blots for ERK1/2 were stripped and re-probed with anti-total ERK antibodies to assess protein loading. The relative intensity of the bands was quantified using transmittance densitometry using Image J software (NIH). The phosphorylated ERK1/2 band densities were normalized for the amount

of total ERK protein for all quantitative analyses. The band densities for L1 in each sample were added, then the density in the LR pool was divided by the total X 100 to calculate the %L1 in LR.

Localization of bilirubin:

Cells were treated for 1 h with 100 μ M HSA with or without 5 μ M bilirubin (B), resulting in four groups: B- MBCD-, B+ MBCD-, B- MBCD+, and B+ MBCD+. LR were isolated from cells from each of the 4 treatment groups. Each fraction of the sucrose gradient was dot blotted for GM1 ganglioside as described above using CTXB and for bilirubin.

Statistical analysis:

Neurite length was determined for the first 30 cells on each coverslip that met the measurement criteria. The mean neurite length for all CGN in each condition per cell preparation was calculated. Descriptive statistics determined the mean \pm standard error of the mean (SEM) of the mean neurite lengths for each condition in each cell preparation. The data was analyzed by ANOVA followed by post hoc pairwise comparison (Tukey) to determine significant differences between treatment groups. $P < 0.05$ was set as significant. For ERK1/2 activation, the ratio of phosphoERK1/2 to total ERK1/2 was calculated for each lane then normalized to the control condition. The relative densitometric units were compared for significance using ANOVA followed by posthoc pairwise comparison, significance defined as $p < 0.05$. %L1 in LR were compared for significance using ANOVA followed by posthoc pairwise comparison (Tukey). For Figure 6, bilirubin presence was dichotomized as yes or no in LR fractions and in non LR fractions and analyzed by Fisher Exact Test.

RESULTS

Bilirubin inhibits L1-mediated neurite outgrowth

CGN grown with L1-Fc showed a significant increase in mean neurite length compared to those grown without L1-Fc (Figure 1). There was a significant decrease in mean neurite length for neurons grown with added L1-Fc after exposure to bilirubin of 5, 10 and 50 μ M (corresponding to Bf of 7.6, 37.6, and 122.5 nM) when compared to the mean neurite length of those neurons grown with L1-Fc and without bilirubin (Figure 1).

Bilirubin has no effect on laminin-mediated neurite outgrowth

CGN grown on laminin showed a significant increase in neurite length when compared to those grown without laminin (Figure 2). Neurons grown on laminin and exposed to bilirubin of 5, 10 and 50 μ M (corresponding to Bf of 7.6, 137.6, and 122.5 nM) did not show a significant change in neurite length when compared to those grown with laminin alone (Figure 2).

L1 activation of ERK1/2 is dependent on LR

The addition of clASCS4 alone showed a significant increase in phosphoERK1/2 compared to control (Figure 3). Treatment with MBCD did not show a significant difference from

the control in the baseline level of phosphoERK1/2 (Figure 3). The addition of 4 mM MBCD for 1 h prior to addition of cIASCs4 prevented the cIASCs4 induced increase in phosphoERK1/2 (Figure 3).

Bilirubin inhibits L1 activation of ERK1/2

The addition of 10 or 50 μ M bilirubin 1 h prior to the addition of cIASCs4 significantly inhibited L1 activation of ERK1/2 compared to treatment with cIASCs4 alone (Figure 4). There were no significant differences between amount of bilirubin added and the amount of phospho-ERK1/2; however, there appeared to be an increasing trend in ERK inhibition in the presence of increasing bilirubin concentrations (Figure 4).

Addition of bilirubin to CGN redistributes L1 in LR.

We have previously shown that a 1 h ethanol treatment significantly increases L1 in LR (25). Therefore, ethanol serves as a positive control for this experiment and significantly increased the percent of L1 in LR. The percent of L1 significantly increased by 2.5 fold in LR with exposure to 5 μ M bilirubin for 1 h (Figure 5).

Localization of bilirubin in LR fractions

When MBCD is absent, GM1 ganglioside was only seen in sucrose density fractions at the upper end of the gradient, fractions 2 – 7 (Figure 6A), indicating these fractions contain LR. Treatment with bilirubin alone did not change which fractions contained GM1 ganglioside, indicating that LR were not dissolved. In the presence of MBCD, the GM1 ganglioside signal was diminished overall and spread throughout the sucrose density gradient indicating LR were dissolved (Figure 6A). Figure 6B shows that only lysates from cells exposed to bilirubin (B+) were immunoreactive for bilirubin indicating specificity of the antibody to bilirubin. In the absence of MBCD, bilirubin was found to be present only in LR containing fractions 2 – 4 (Figure 6B). In the presence of MBCD, bilirubin immunoreactivity was diminished and spread through all fractions.

DISCUSSION

In summary, within the physiologic range, bilirubin, and presumptively Bf 1) inhibits L1-but not laminin-mediated neurite outgrowth, 2) inhibits L1 activation of ERK1/2, 3) causes a redistribution of L1 into LR, and 4) binds only to LR. These results suggest that one potential mechanism of the neurotoxicity of bilirubin is the dysfunction of LR.

The interaction of bilirubin with neuronal membranes is not a new finding. Initially described by Mustafa et al (37), attention was focused on mitochondrial membranes and the inhibition of oxidative phosphorylation. However, an early study showed no effect of bilirubin on oxidative phosphorylation coupling in animals with bilirubin encephalopathy (38). Bilirubin oxidizes membrane phospholipids, but this effect does not account for all the activity of bilirubin (39). Nakai and Kamiguchi demonstrated that GM1 ganglioside was integral in LR and only associated with lipid raft fractions (40). Interestingly, low levels of bilirubin have been shown to ameliorate the effects of oxidative stress on GM1 ganglioside

redistribution (41). In this study, we demonstrated the increased concentration of bilirubin did not alter the distribution of GM1 ganglioside.

Bilirubin has previously been shown to inhibit ERK1/2 activation by other proteins. Bilirubin inhibited NGF and BDNF activation of ERK1/2 in PC12 and primary rat CGN (42). In addition, others have demonstrated the necessity of ERK1/2 in the bilirubin-induced apoptosis pathway, which coincides with our findings (43). Bilirubin-mediated inhibition of neointimal thickening was also accompanied by significant decreases in ERK1/2 signaling, further supporting our findings of bilirubin-inhibited ERK1/2 activation (44). Bilirubin has been shown to activate ERK1/2, but only in HRT-18 (colon cancer) cells, which likely utilize ERK1/2 in separate pathways (45).

The Bf concentrations of 7.6 and 37.6 nM in this study are within the range measured clinically (46,47). Elevated Bf is associated with bilirubin-induced neurotoxicity, as it is able to cross the blood brain barrier (48). In addition, preterm neonates are more susceptible to bilirubin neurotoxicity, despite lower levels of total serum bilirubin (both bound and unbound) (49); therefore, the focus of this study is to examine the effects of unbound bilirubin at concentrations including ones in the physiologic range. The measurement of Bf is not routinely used in clinical management, nor is the assay routinely available in clinical laboratories (48). Several of the methods for measuring Bf are in dispute. A recent large clinical trial utilizes the total serum bilirubin/albumin (B/A) ratio as a proxy for Bf due to the lack of reliable assay methods (48). Our albumin concentration was 100 μ M and our bilirubin to albumin molar ratio was varied from 1:2 to 1:100 in these studies. One possible limitation of this study is that the bilirubin used was not purified before use. We use measurements of Bf from less than the limit of detection (i.e., lower than 7.6 nM) to 122 nM, spanning beyond the range of Bf in preterm infant blood, given that the physiologic range of Bf is at 70 nM (Ostrow, 2004).

Bilirubin may insert itself into the membrane disrupting the ability of proteins to traffic in and out of the LR. This dysfunction may occur without dissolving LR entirely. Subtle alterations in the membrane composition can alter the ability of membranes to be in an ordered (LR) or disordered state (non-LR), which would alter the ability of a protein to associate with LR. These interrupted protein-lipid interactions can have detrimental effects on cerebellar development and lead to profound neuronal damage. LR were first described in the early 1990's, but their existence was debated for two decades (14). A body of literature now supports their existence as dynamic membrane domains, rapidly aggregating and disaggregating to bring molecules involved in signaling together, then apart. Neuronal proteins are either constitutive elements of the LR, excluded from the LR, or trafficked through the LR. The function of some proteins is altered whether they are within or out of the LR (19). L1 is an example of a protein that traffics through the LR (25). L1 cannot stay in the LR and be functional; it must traffic through LR while undergoing a series of phosphorylation/dephosphorylation events. Bf is causing either enhanced trafficking of L1 to LR or retarding the movement of L1 out of LR, both would result in an increase of L1 in the LR. We compared the effect of bilirubin on two neurite outgrowth pathways: one involving L1 (and therefore LR), and one involving laminin, which do not use LR (24). Our results show that bilirubin effects LR dependent neurite outgrowth (Figure 1), and does not affect

LR independent neurite outgrowth (Figure 2). These results suggest that LR are a target for bilirubin in the cerebellum. We are actively investigating the in vivo effects of bilirubin on the cerebellum using our Gunn Rat model of preterm hyperbilirubinemia.

The identification of LR function as a target for bilirubin may open the door to different interventions to prevent neurotoxicity. The integrity of LR is determined by the ratio of sphingomyelin to phosphatidylcholine, for which choline is a known precursor. Choline supplementation is being actively investigated to prevent and/or reverse the effects of ethanol in animal models of fetal alcohol spectrum disorder (50–54). It has been proposed that 25% of pregnant women are choline deficient (55). Therefore, certain infants may have altered sphingomyelin to phosphatidylcholine ratios, making their LR more susceptible to damage and altered function. Supplementation with choline may restore resilience of the LR to lipophilic substances like ethanol and bilirubin. Supplementation with GM1 ganglioside, another constituent of LR, may be another interventional strategy. GM1 ganglioside has been tested for its ability to reduce the progression of Parkinson's disease (56).

Bilirubin-induced neuronal dysfunction remains a significant clinical problem. Phototherapy significantly reduces total serum bilirubin concentration and reduces the number of exchange transfusions, but it does not improve outcomes (57) possibly because it does not reduce Bf levels to concentrations that have no neurotoxicity. Minocycline reduces bilirubin-induced neurological dysfunction in animal models (58), but its side effects make it unsuitable for use in neonates. Better interventions are needed.

In sum, our results suggest that bilirubin interferes with normal LR function, and suggests a new therapeutic target to prevent or reduce bilirubin neurotoxicity.

Acknowledgements:

This material is original and has not been previously published nor has it been submitted for publication elsewhere while under consideration.

This study was funded by NIH R01AA016398 and R21HD085061, Rockville, MD (CB) and the Cobey Endowment, Baltimore, MD (CB) and The Munro Fund, Baltimore, MD (CB).

We would like to acknowledge the special contributions of Sean Sukys, Hemal N. Sempat, and Nicholas Rickman.

REFERENCES

1. Shapiro SM, Nakamura H. Bilirubin and the auditory system. *J Perinatol* 2001;21 Suppl 1:S52–5; discussion S59–62. [PubMed: 11803418]
2. Arnold C, Pedroza C, Tyson JE. Phototherapy in ELBW newborns: does it work? Is it safe? The evidence from randomized clinical trials. *Semin Perinatol* 2014;38:452–64. [PubMed: 25308614]
3. Xoinis K, et al. Extremely low birth weight infants are at high risk for auditory neuropathy. *J Perinatol* 2007;27:718–23. [PubMed: 17703185]
4. Biran V, Verney C, Ferriero DM. Perinatal cerebellar injury in human and animal models. *Neurol Res Int* 2012;2012:858929. [PubMed: 22530126]
5. Bhutani VK, Wong RJ, Stevenson DK. Hyperbilirubinemia in Preterm Neonates. *Clin Perinatol* 2016;43:215–32. [PubMed: 27235203]
6. Amin SB, Lamola AA. Newborn jaundice technologies: unbound bilirubin and bilirubin binding capacity in neonates. *Semin Perinatol* 2011;35:134–40. [PubMed: 21641486]

7. Malik SG, Irwanto KA, Ostrow JD, Tiribelli C. Effect of bilirubin on cytochrome c oxidase activity of mitochondria from mouse brain and liver. *BMC Res Notes* 2010;3:162. [PubMed: 20534120]
8. Ahlfors CE. Predicting bilirubin neurotoxicity in jaundiced newborns. *Curr Opin Pediatr* 2010;22:129–33. [PubMed: 20125026]
9. Shapiro SM. Definition of the clinical spectrum of kernicterus and bilirubin-induced neurologic dysfunction (BIND). *J Perinatol* 2005;25:54–9. [PubMed: 15578034]
10. Ostrow JD, Pascolo L, Tiribelli C. Reassessment of the unbound concentrations of unconjugated bilirubin in relation to neurotoxicity in vitro. *Pediatr Res* 2003;54:98–104. [PubMed: 12646712]
11. Danbolt C, et al. In vitro binding of [3H]bilirubin to neurons in rat brain sections. *Biol Neonate* 1993;63:35–9. [PubMed: 8443292]
12. Ostrow JD, Pascolo L, Brites D, Tiribelli C. Molecular basis of bilirubin-induced neurotoxicity. *Trends Mol Med* 2004;10:65–70. [PubMed: 15102359]
13. Mukerjee P, Ostrow JD. Interactions of unconjugated bilirubin with vesicles, cyclodextrins and micelles: New modeling and the role of high pKa values. *BMC Biochem* 2010;11:15. [PubMed: 20350305]
14. Simons K, Gerl MJ. Revitalizing membrane rafts: new tools and insights. *Nat Rev cell Biol* 2010;11:688–99.
15. Patel HH, Murray F, Insel PA. Caveolae as organizers of pharmacologically relevant signal transduction molecules. *Annu Rev Pharmacol Toxicol* 2008;48:359–91. [PubMed: 17914930]
16. Epshtein Y, et al. Identification of a C-terminus domain critical for the sensitivity of Kir2.1 to cholesterol. *Proc Natl Acad Sci U S A* 2009;106:8055–60. [PubMed: 19416905]
17. Fantini J, Barrantes FJ. Sphingolipid/cholesterol regulation of neurotransmitter receptor conformation and function. *Biochim Biophys Acta* 2009;1788:2345–61. [PubMed: 19733149]
18. Simons K, Ikonen E. Functional rafts in cell membranes. *Nature* 1997;387:569–72. [PubMed: 9177342]
19. Dart C Lipid microdomains and the regulation of ion channel function. *J Physiol* 2010;588:3169–78. [PubMed: 20519314]
20. Simons K, Ehehalt R. Cholesterol, lipid rafts, and disease. *J Clin Invest* 2002;110:597–603. [PubMed: 12208858]
21. Owen DM, Magenau A, Williamson D, Gaus K. The lipid raft hypothesis revisited--new insights on raft composition and function from super-resolution fluorescence microscopy. *Bioessays* 2012;34:739–47. [PubMed: 22696155]
22. Korade Z, Kenworthy AK. Lipid rafts, cholesterol, and the brain. *Neuropharmacology* 2008;55:1265–73. [PubMed: 18402986]
23. Pike LJ. The challenge of lipid rafts. *J Lipid Res* 2009;50 Suppl:S323–8. [PubMed: 18955730]
24. Nakai Y, Kamiguchi H. Migration of nerve growth cones requires detergent-resistant membranes in a spatially defined and substrate-dependent manner. *J Cell Biol* 2002;159:1097–108. [PubMed: 12499360]
25. Tang N, et al. Ethanol causes the redistribution of L1 cell adhesion molecule in lipid rafts. *J Neurochem* 2011;119:859–67. [PubMed: 21884525]
26. Kamiguchi H, Lemmon V. Recycling of the cell adhesion molecule L1 in axonal growth cones. *J Neurosci* 2000;20:3676–86. [PubMed: 10804209]
27. Schmid RS, Pruitt WM, Maness PF. A MAP kinase-signaling pathway mediates neurite outgrowth on L1 and requires Src-dependent endocytosis. *J Neurosci* 2000;20:4177–88. [PubMed: 10818153]
28. Yeane NK, et al. Ethanol inhibits L1 cell adhesion molecule tyrosine phosphorylation and dephosphorylation and activation of pp60(src). *J Neurochem* 2009;110:779–90. [PubMed: 19457108]
29. Watanabe H, et al. Phospholipase D2 functions as a downstream signaling molecule of MAP kinase pathway in L1-stimulated neurite outgrowth of cerebellar granule neurons. *J Neurochem* 2004;89:142–51. [PubMed: 15030398]
30. Milstone AM, et al. Chlorhexidine inhibits L1 cell adhesion molecule-mediated neurite outgrowth in vitro. *Pediatr Res* 2014;75:8–13. [PubMed: 24126818]

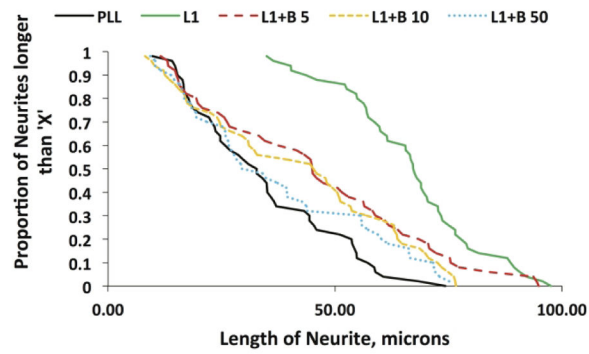
31. Tang N, et al. Choline partially prevents the impact of ethanol on the lipid raft dependent functions of I1 cell adhesion molecule. *Alcohol Clin Exp Res* 2014;38:2722–30. [PubMed: 25421509]
32. Gonzalez-Reyes S, et al. Neuroprotective role of heme-oxygenase 1 against iodoacetate-induced toxicity in rat cerebellar granule neurons: Role of bilirubin. *Free Radic Res* 2009;43:214–23. [PubMed: 19177228]
33. Ahlfors CE. Measurement of plasma unbound unconjugated bilirubin. *Anal Biochem* 2000;279:130–5. [PubMed: 10706781]
34. Shapiro SM, Sombati S, Geiger A, Rice AC. NMDA channel antagonist MK-801 does not protect against bilirubin neurotoxicity. *Neonatology* 2007;92:248–57. [PubMed: 17556843]
35. Bearer CF, Swick AR, O’Riordan MA, Cheng G. Ethanol inhibits L1-mediated neurite outgrowth in postnatal rat cerebellar granule cells. *J Biol Chem* 1999;274:13264–70. [PubMed: 10224086]
36. Tang N, et al. Ethanol inhibits L1 cell adhesion molecule activation of mitogen-activated protein kinases. *J Neurochem* 2006;96:1480–90. [PubMed: 16478533]
37. Mustafa MG, King TE. Binding of bilirubin with lipid. A possible mechanism of its toxic reactions in mitochondria. *J Biol Chem* 1970;245:1084–9. [PubMed: 5461380]
38. Diamond I, Schmid R. Oxidative phosphorylation in experimental bilirubin encephalopathy. *Science* 1967;155:1288–9. [PubMed: 6018655]
39. Daood MJ, Hoyson M, Watchko JF. Lipid peroxidation is not the primary mechanism of bilirubin-induced neurologic dysfunction in jaundiced Gunn rat pups. *Pediatr Res* 2012;72:455–9. [PubMed: 22902434]
40. Nakai Y, Kamiguchi H. Migration of nerve growth cones requires detergent-resistant membranes in a spatially defined and substrate-dependent manner. *J Cell Biol* 2002;159:1097–108. [PubMed: 12499360]
41. Šmíd V, et al. Heme oxygenase-1 may affect cell signalling via modulation of ganglioside composition. *Oxid Med Cell Longev* 2018;2018.
42. Mancuso C, et al. Bilirubin as an endogenous modulator of neurotrophin redox signaling. *J Neurosci Res* 2008;86:2235–49. [PubMed: 18338802]
43. Fernandes A, et al. MAPKs are key players in mediating cytokine release and cell death induced by unconjugated bilirubin in cultured rat cortical astrocytes. *Eur J Neurosci* 2007;25:1058–68. [PubMed: 17331202]
44. Peyton KJ, et al. Bilirubin inhibits neointima formation and vascular smooth muscle cell proliferation and migration. *Front Pharmacol* 2012;3 MAR:1–8. [PubMed: 22291651]
45. Öllinger R, et al. Bilirubin inhibits tumor cell growth via activation of ERK. *Cell Cycle* 2007;6:3078–85. [PubMed: 18073533]
46. Lee YK, et al. The significance of measurement of serum unbound bilirubin concentrations in high-risk infants. *Pediatr Int* 2009;51:795–9. [PubMed: 19419529]
47. van der Schoor LW, et al. Unconjugated free bilirubin in preterm infants. *Early Hum Dev* 2017;106–107:25–32.
48. Hulzebos CV, et al. The bilirubin albumin ratio in the management of hyperbilirubinemia in preterm infants to improve neurodevelopmental outcome: a randomized controlled trial--BARTrial. *PLoS One* 2014;9:e99466. [PubMed: 24927259]
49. Amin SB, Wang H. Bilirubin Albumin Binding and Unbound Unconjugated Hyperbilirubinemia in Premature Infants. *J Pediatr [Internet]* 2018;192:47–52. Available from: 10.1016/j.jpeds.2017.09.039
50. Bearer CF, et al. Choline Ameliorates Deficits in Balance Caused by Acute Neonatal Ethanol Exposure. *Cerebellum* 2015;14:413–20. [PubMed: 26085462]
51. Davis NL, et al. Choline ameliorates ethanol induced alterations in tyrosine phosphorylation and distribution in detergent-resistant membrane microdomains of L1 cell adhesion molecule in vivo. *Birth Defects Res* 2020;1–10.
52. Monk BR, Leslie FM, Thomas JD. The effects of perinatal choline supplementation on hippocampal cholinergic development in rats exposed to alcohol during the brain growth spurt. *Hippocampus* 2012;22:1750–7. [PubMed: 22431326]

53. Thomas JD, Idrus NM, Monk BR, Dominguez HD. Prenatal choline supplementation mitigates behavioral alterations associated with prenatal alcohol exposure in rats. *Birth defects Res A, Clin Mol Teratol* 2010;88:827–37. [PubMed: 20706995]
54. Waddell J, Mooney SM. Choline and working memory training improve cognitive deficits caused by prenatal exposure to ethanol. *Nutrients* 2017;9.
55. Zeisel SH. Nutrition in pregnancy: the argument for including a source of choline. *Int J Womens Health* 2013;5:193–9. [PubMed: 23637565]
56. Schneider JS, et al. Parkinson's disease: improved function with GM1 ganglioside treatment in a randomized placebo-controlled study. *Neurology* 1998;50:1630–6. [PubMed: 9633704]
57. Kalpoyiannis N, et al. Efficacy of phototherapy and/or exchange transfusions in neonatal jaundice. *Clin Pediatr (Phila)* 1982;21:602–6. [PubMed: 7116744]
58. Geiger AS, Rice AC, Shapiro SM. Minocycline blocks acute bilirubin-induced neurological dysfunction in jaundiced Gunn rats. *Neonatology* 2007;92:219–26. [PubMed: 17556840]

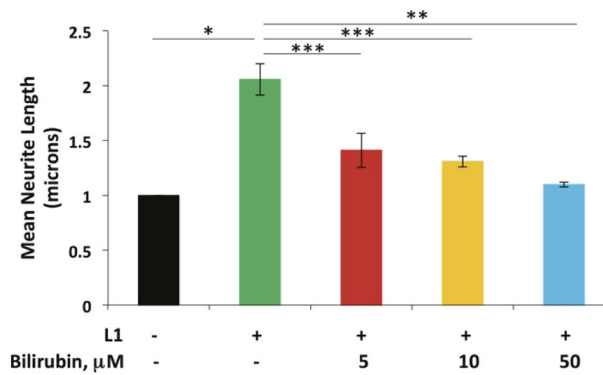
Impact Statement:

- This article establishes lipid rafts as a target for the neurotoxic effects of bilirubin.
- This article provides clear evidence toward establishing one mechanism of bilirubin neurotoxicity, where little is understood.
- This article paves the way for future investigation into lipid raft dependent functions, and its role in neurodevelopmental outcome.

1A

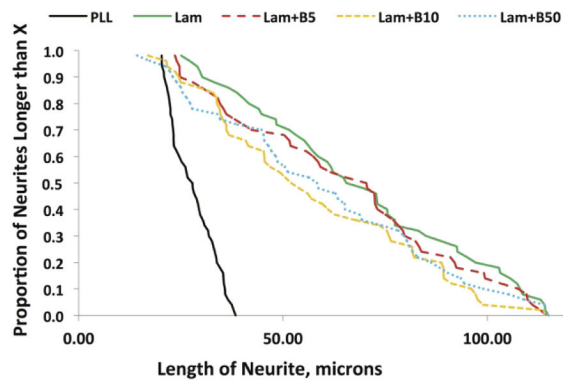


B

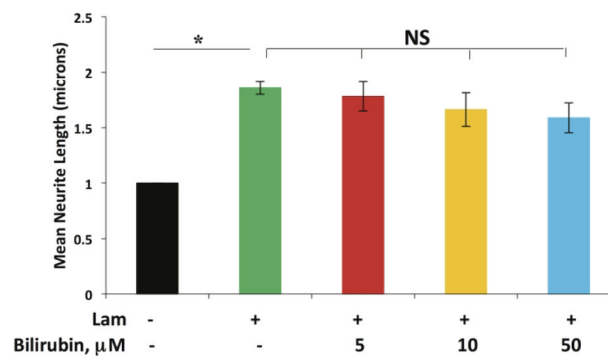
**Figure 1.**

Bilirubin inhibits L1 mediated neurite outgrowth at physiologic concentrations of Bf. A. Distribution curve of neurite lengths without L1, L1, or L1 plus 5, 10, or 50 μM of bilirubin from a representative experiment. B. Bar graph of mean \pm SEM neurite lengths of CGN grown without L1, L1, or L1 plus 5, 10, or 50 μM of bilirubin normalized to CGN grown on PLL alone. L1 significantly increases neurite length, and all concentrations of bilirubin tested significantly reduce the mean neurite length relative to the L1 alone group. $N=3$, ANOVA $p<0.001$, posthoc pairwise comparison (Tukey) * $p<0.0001$; ** $p<0.001$; † $p<0.01$

2A

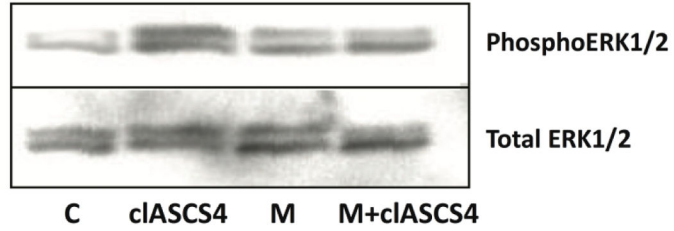


B

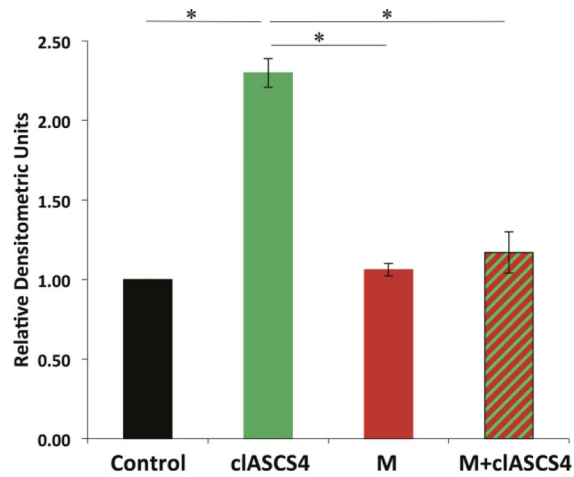
**Figure 2.**

Bilirubin does not inhibit laminin-mediated neurite outgrowth at physiologic concentrations of Bf. A. Distribution curve of neurite lengths with PLL alone, laminin (Lam), or Lam plus 5, 10, or 50 μM of bilirubin from a representative experiment. B. Bar graph of mean \pm SEM neurite lengths of CGN grown without Lam, Lam, or Lam plus 5, 10, or 50 μM of bilirubin normalized to CGN grown on PLL alone. $N=3$, ANOVA $p<0.01$, posthoc pairwise comparison (Tukey), $*p<0.01$, NS = non significant.

3A

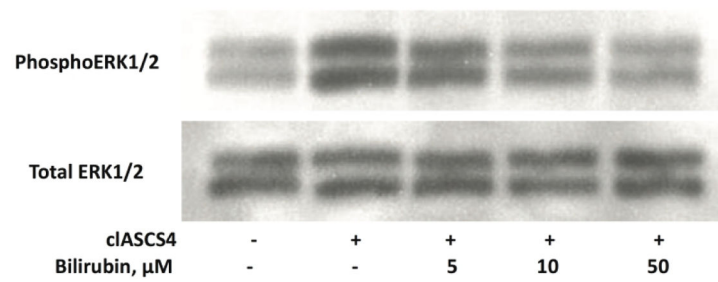


B

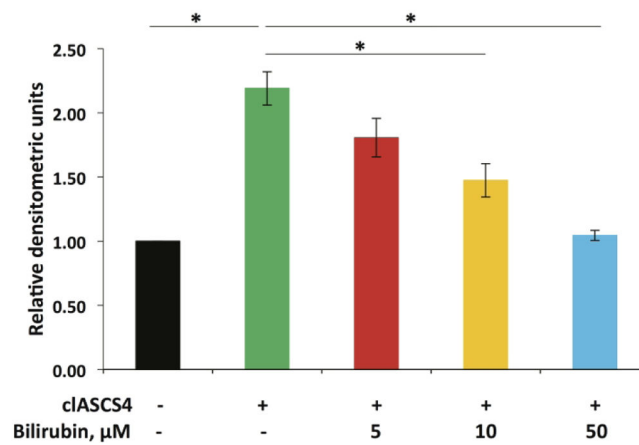
**Figure 3.**

L1 activation of ERK1/2 is dependent on lipid rafts. A. A representative immunoblot of phosphoERK1/2 and total ERK with and without MBCD (M). The experimental groups are as follows: Mouse IgG (C); cIASCS4; MBCD added 1 h prior Mouse IgG alone (M); MBCD added 2 h prior to cIASCS4 (M+L1). B. Bar graph of mean \pm SEM of relative densitometric units of phosphoERK1/2 and total ERK, normalized to the control, N = 3, ANOVA $p < 0.0001$, posthoc pairwise comparison (Tukey) $*p < 0.01$

4A

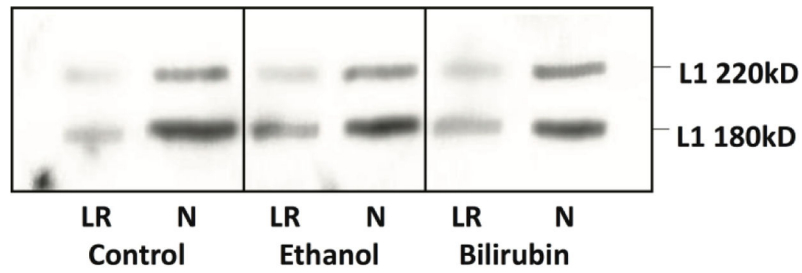


B

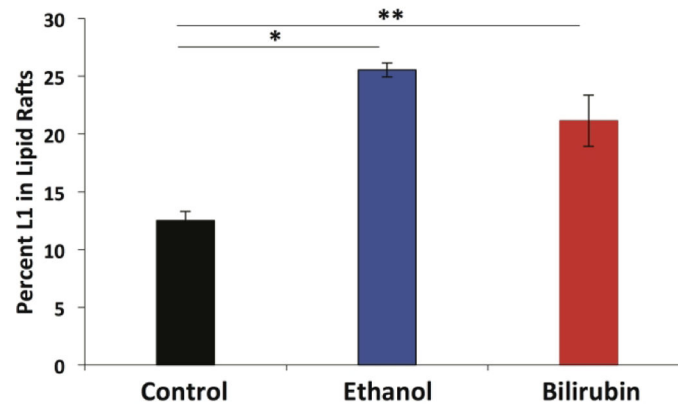
**Figure 4.**

Physiologic bilirubin concentrations inhibit L1 activation of ERK1/2. A. A representative immunoblot of phosphoERK1/2 with total ERK as a loading control. CGN treated without cIASC4, cIASC4, or cIASC4 plus 5, 10, or 50 μM bilirubin as indicated for 1 h prior to addition of cIASC4. B. Bar graph of mean \pm SEM of relative densitometric units of cIASC4 activation of ERK1/2 normalized to control. N = 3, ANOVA $p < 0.0001$, posthoc pairwise comparison (Tukey) $*p < 0.01$

5A

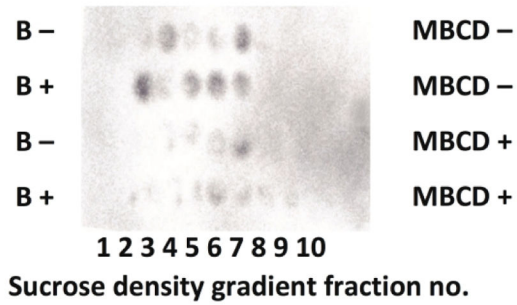


B

**Figure 5.**

The fraction of total L1 in the lipid raft pool is increased by bilirubin. A. Representative immunoblot showing L1 distribution in lipid rafts (LR) and non-lipid rafts (N) in K5 media alone (control), the presence of 25 mM ethanol (EtOH) as a positive control, or 5 μ M bilirubin. B. Bar graph of %L1 in lipid rafts (LR*100/(LR+N)) (mean \pm SEM). N=3, ANOVA $p < 0.01$, posthoc pairwise comparison (Tukey) * $p < 0.01$, ** $p < 0.05$

6A



B

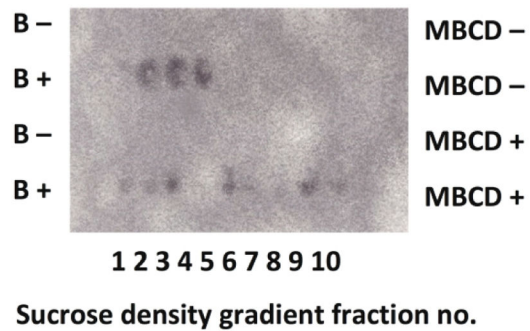


Figure 6. Bilirubin is found only in lipid raft containing fractions of a sucrose density gradient. A. Representative dot blot of sucrose gradients treated with bilirubin and/or MBCD and reactive to CTXB. B. Representative dot blot of the same fractions immunoreactive with bilirubin.